

VENTRICULAR FUNCTION

Impact of the ECG gating method on ventricular volumes and ejection fractions assessed by cardiovascular magnetic resonance imaging

BURKHARD SIEVERS, M.D.,* MARVIN ADDO, SIMON KIRCHBERG, ASLI BAKAN, BINU JOHN-PUTHENVEETIL, ULRICH FRANKEN, M.D., and HANS-JOACHIM TRAPPE, M.D.

Department of Cardiology and Angiology, Marienhospital, University of Bochum, Herne, NRW, Germany

Purpose. Most MRI centers currently use prospective ECG triggering and fast gradient-echo sequences for image acquisition. Retrospectively gated sequences allow the coverage of the entire cardiac cycle. There is concern about whether ventricular volumes and ejection fraction (EF) differ according to the gating method used for image acquisition. We sought to evaluate the impact of the gating method on measurements of right and left ventricular volumes and EF in normal subjects. **Materials and Methods.** Fifteen subjects with no cardiovascular disease were investigated by MRI using a 1.5 Tesla scanner. Images were acquired with a gradient-echo sequence with steady-state free precession (SSFP) using the standard short-axis method for volume and EF measurements. Images were acquired with 6-mm-thick slices using both prospective triggering and retrospective gating. Left and right ventricular volumes (EDV, ESV, SV) and EF were determined with a commercially available software package (Argus, Siemens). **Results:** EDV and SV calculated from short-axis images were significantly smaller with the prospectively triggered SSFP sequence (mean difference: EDV left: 13.9 ± 4.4 mL, $p < 0.0001$; SV left: 13.5 ± 4.8 mL, $p < 0.0001$; EDV right: 14.2 ± 3.9 mL, $p < 0.0001$; SV right: 14.7 ± 5.9 mL, $p < 0.0001$). EF was significantly smaller for the right ventricle (mean difference $-3.6 \pm 3.3\%$, $p = 0.0008$) and the left ventricle (mean difference $-2.3 \pm 3.3\%$, $p = 0.02$). ESV remained unchanged (mean difference: ESV left: 0.47 ± 3.5 mL, $p = 0.6179$; right ESV: 0.5 ± 3.7 mL, $p = 0.6083$). **Conclusion.** The gating method has a significant impact on volume and EF measurements. The global ventricular EF is underestimated by using the prospective triggering technique. However, the difference in the left ventricle is small and might not be of clinical relevance.

Key Words: Cardiovascular magnetic resonance imaging; Steady-state free precession gradient echo sequence (SSFP); Prospective ECG triggering; Retrospective gating; Ventricular volumes; Ventricular ejection fractions

1. Introduction

Most MRI centers use prospectively triggered gradient-echo sequences for ventricular volume and EF assessment. Recently published reference values for MRI assessment of ventricular volumes and EF are based on calculations from short-axis images acquired with prospectively triggered sequences (1, 2). It is known that prospectively triggered sequences do not cover the entire cardiac cycle because the acquisition window is set 10–20% below the average cardiac cycle length (Fig. 1A). Therefore, the late diastole of each cardiac cycle is not entirely covered. Thus, end-diastolic volumes might be underestimated by this trigger technique.

In prospectively triggered gradient-echo sequences, the same slice position is excited with a fixed number of radio-frequency (RF) pulses. The number of phases depends on the TR and the heart rate. After a fixed number of excitations per RR-interval, the system waits for the next R-wave, leaving out the late diastole of the cardiac cycle. In gradient-echo sequences with steady-state free precession, such as TrueFISP, this gap of data points in the late diastole usually disturbs the steady state and leads to an increased signal intensity (lightening artifact) in the first images of each cine set (3). This can be avoided by implementing dummy pulses to bridge the gap between the last and the next excitation pulse. Dummy pulses maintain the steady state, although no data points are acquired during this time.

Retrospectively gated gradient-echo sequences cover the entire cardiac cycle, including the late diastole and thus are supposed to be more accurate in volume and EF assessment than prospectively triggered sequences. There are two ways to accomplish the data acquisition: first, by switching to the next segment after each R-wave and second, by collecting enough data for every segment to entirely cover even the longest

Received 18 June 2004; accepted 25 August 2004.

*Address correspondence to Burkhard Sievers, M.D., Duke Cardiovascular Magnetic Resonance Center, Duke University Medical Center, Duke Clinic, RM 00354, SB, Orange Zone, Trent Drive, DUMC 3934, Durham, NC 27710, USA. Fax: (919) 668-5588; E-mail: burkhard.sievers@gmx.de

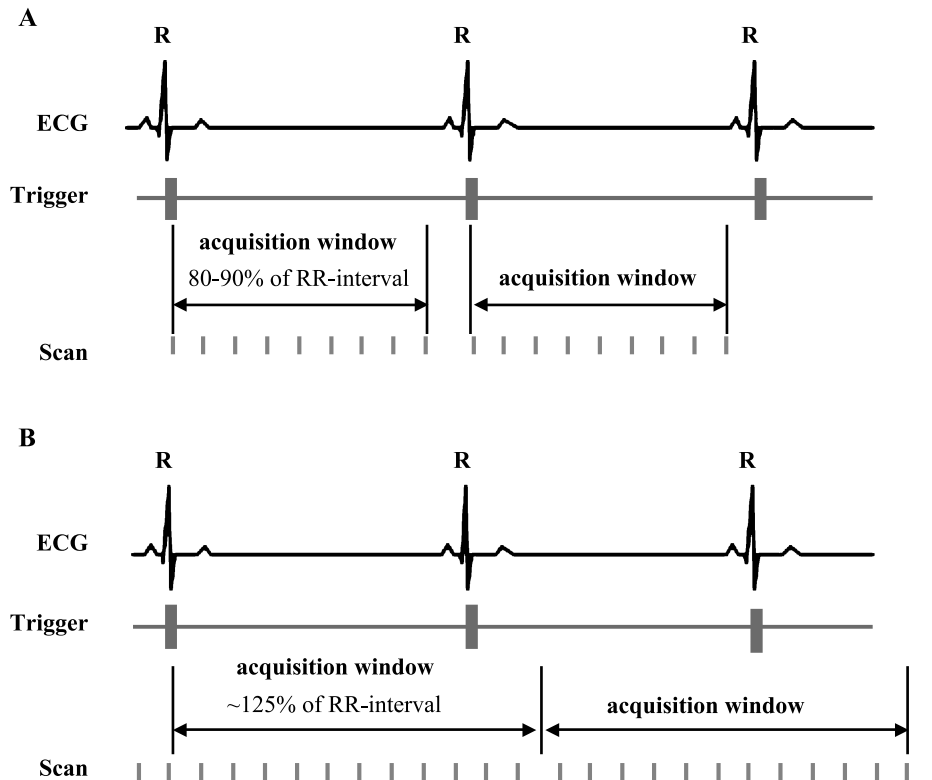


Figure 1. Timing diagram of the prospectively triggered SSFP sequence (A) and the retrospectively gated SSFP sequence (B).

cardiac cycle. In the first method, a variable number of time frames for each segment is acquired depending on the cardiac cycle length. Each cardiac cycle is completely covered by only one particular segment. It requires flexibility to switch to the new segment on the fly.

In the second method, a fixed number of time frames is sampled, which is technically easier to implement (3). An arbitrary number of images can be reconstructed in the cine series because data interpolation is used to generate images at any time point in the cardiac cycle. The image acquisition is asynchronous with the ECG. The length of time for each phase-encoding step is set by the acquisition window. A time stamp indicating the time relative to the previous R-wave is stored with each phase-encoding step. The acquisition window is defined to be longer than the maximum RR-interval to ensure data acquisition for each part of the cardiac cycle (Fig. 1B). After the acquisition, the data are sorted based on time stamps that indicate the time to the previous R-wave, and reconstructed into a series of images covering the entire cardiac cycle. We used the second approach where a fixed number of time frames was sampled. At the time the study was performed this was the only available retrospectively gated gradient-echo cine sequence.

Retrospectively gated cine imaging has been shown to have less sensitivity to artifacts such as blurring and lightening, and is less sensitive to irregular heart rates (3). The disadvantage of the retrospectively gated acquisition is the longer scan time compared to prospective triggered acquisition. The reason is

that the acquisition window needs to be set at 125% of the average cardiac cycle length.

We sought to study the impact of the gating method on measurements of ventricular volumes and EF in normal subjects.

2. Materials and methods

The study was prospectively planned and was approved by the local Institutional Review Board. Written consent was obtained in all cases.

Fifteen consecutive subjects with no prior history of cardiovascular pathology (seven women and eight men, mean age 52.9 ± 11.2 years) underwent MRI for the evaluation of cardiac function and the determination of cardiac volumes and EF using 6-mm-thick slices. All images were acquired in the same examination. Heart disease was excluded in all subjects before MRI by noninvasive diagnostic techniques (ECG, chest X-ray, treadmill exercise ECG, echocardiography, thallium myocardial scintigraphy). None of the subjects included in the study had a history of hypertension and diabetes. The mean heart rate was 65 ± 13 bpm.

2.1. Image acquisition

MRI was performed with a 1.5 Tesla Scanner (Sonata, Magnetom, Siemens, Erlangen, Germany) using an anterior

Table 1. Displayed are the left and right ventricular volumes and EF calculated from retrospective gated and prospective triggered SSFP images, the mean difference, and the 95% limits of agreement

Mean \pm SD	Retrospectively gating	Prospectively triggering	Mean difference	P-value	95% limits of agreement
Left ventricle					
EDV [mL]	131.2 \pm 21.3	117.2 \pm 18.1	-13.9 \pm 4.4	< 0.0001	-22.7, -5.1
ESV [mL]	32.2 \pm 7.8	31.7 \pm 8.9	-0.47 \pm 3.5	0.62	-7.5, 6.5
SV [mL]	99.0 \pm 19.2	85.5 \pm 16.0	-13.5 \pm 4.8	< 0.0001	-23.1, -3.9
EF [%]	75.3 \pm 5.0	72.7 \pm 7.2	-2.3 \pm 3.3	0.02	-8.9, 4.3
Right ventricle					
EDV [mL]	137.1 \pm 36.4	122.9 \pm 33.7	-14.2 \pm 3.9	< 0.0001	-22.0, -6.4
ESV [mL]	41.9 \pm 14.4	42.4 \pm 16.0	0.5 \pm 3.7	0.61	-6.9, 7.9
SV [mL]	95.2 \pm 23.7	80.5 \pm 19.2	-14.7 \pm 5.9	< 0.0001	-26.5, -2.9
EF [%]	69.8 \pm 4.4	66.2 \pm 5.2	-3.6 \pm 3.3	0.0008	-10.2, 3.0

Abbreviations: EDV = end-diastolic volume; ESV = end-systolic volume; SV = stroke volume; EF = ejection fraction.

and posterior surface coil array (CP Body Array Flex, CP Spine Array, Siemens) and prospective as well as retrospective ECG triggering. The dimensions of the coil elements are about 160 mm in the z-direction (head to feet) and about 460 mm in the x-direction (right to left). **A fast imaging sequence with steady-state free precession (SSFP)** and constant radio-frequency pulsing was used (4).

On the basis of scout images, cine images were acquired in the short axis and horizontal and vertical long axes. Short-axis images were acquired from the base of the heart (atrioventricular ring) to the apex with **6-mm-thick slices (4-mm interslice gap)** during breath holding in end-expiration using a fast gradient-echo sequence (SSFP) with both prospective and retrospective ECG triggering. We used 6-mm-thick slices to avoid major influences by partial volume effects. A 4-mm interslice gap was used to allow coverage of the ventricles in 10-mm steps.

Parameters for the prospectively triggered SSFP sequence: temporal resolution = 39 ms, echo time = 1.5 ms, slice thickness = 6 mm, inter-slice gap = 4 mm, FoV read 380 mm, FoV phase 78%, base resolution 256, phase resolution 62%, flip angle = 65°, in-plane pixel size = 2.4 \times 1.5 mm, matrix 124 \times 256 pixel, number of cardiac phases = 16 (depending on heart rate), number of segments = 13,

bandwidth 977 Hz/Px, scan time = 8–10 sec, depending on the heart rate.

Parameters for the retrospectively gated SSFP: temporal resolution = 42 ms, echo time = 1.4 ms, slice thickness = 6 mm, inter-slice gap = 4 mm, FoV read 380 mm, FoV phase 78%, base resolution 192, phase resolution 70%, flip angle = 65°, in-plane pixel size = 2.8 \times 2.0 mm, matrix 105 \times 192 pixel, number of cardiac phases = 28, calculated phases = 25, number of segments = 15, bandwidth 930 Hz/Px, scan time = 11–14 sec, depending on the heart rate.

2.2. Image analysis

Images were analyzed blinded and in a random order with a commercially available computer software Argus (Siemens) by an experienced observer (BS). All patient identifiers and image parameters were removed from the images before analysis. Published criteria were used for the delineation of cardiac borders (5). **Papillary muscles and trabeculations were excluded for volume measurements.** Contour tracing was aided by reviewing the multiple phase scans in the cine mode. For both left and right ventricular volume assessment, end-diastole was defined visually as the phase with the largest volume, and end-systole as the phase with the smallest

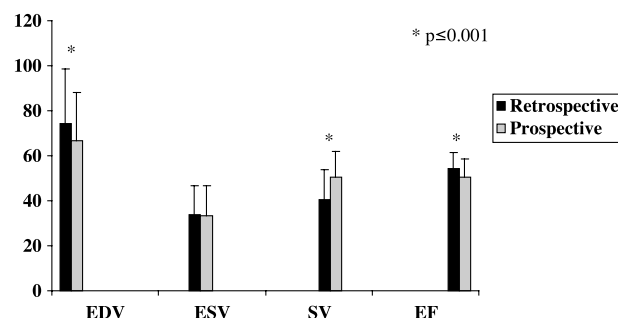


Figure 2. Mean and standard deviations of left and right ventricular volumes and EF, displayed as boxplots. EDV, SV, and EF differ significantly according to the gating technique used for image acquisition.

volume (the cardiac phase with minimal cross-sectional diameter). At the base of the heart, slices were considered to be in the left ventricle if the blood was at least half-surrounded by ventricular myocardium. For the basal slice the contours were traced up to the junction of the atrium and the ventricle. Blood volume up to the aortic valve was included in the left ventricular volume. Only the blood volume below the level of the pulmonary valve was included for right ventricular volume assessment. The epicardium and endocardium of the left ventricle and the endocardium of the right ventricle were traced in each end-diastolic and end-systolic slice and the sum of the marked areas used to calculate the total volume. Ventricular end-diastolic volume (EDV) and end-systolic volume (ESV) were calculated from the sum of the outlined areas using the Simpson's rule. Stroke volumes (SV) and ejection fractions (EF) were calculated from the formula $SV = EDV - ESV$ and $EF = SV/EDV \times 100\%$.

To assess interobserver variability of the measurements, a second blinded observer (SK) measured the same data set, unaware of the results of the other observer.

2.3. Statistical analysis

Mean and standard deviations (SD) were derived for each of the parameters. The differences in calculated volumes and EF using different gating methods were assessed by using paired t-test. All statistical tests were two tailed, p-value less than 0.05 was regarded as significant. Interobserver variability was defined with the formula $(\text{observer A} - \text{observer B}) / (\text{mean observer A and B})$. Bland-Altman plots were performed from the measurements obtained by the two observers (6).

3. Results

Differences in left and right ventricular volumes and EF are displayed in Table 1 and Fig. 2. EDV and SV calculated from short-axis images were significantly smaller with the prospectively gated SSFP sequence than with the prospectively triggered sequence (mean difference: EDV left: 13.9 ± 4.4 mL, $p < 0.0001$; SV left: 13.5 ± 4.8 mL,

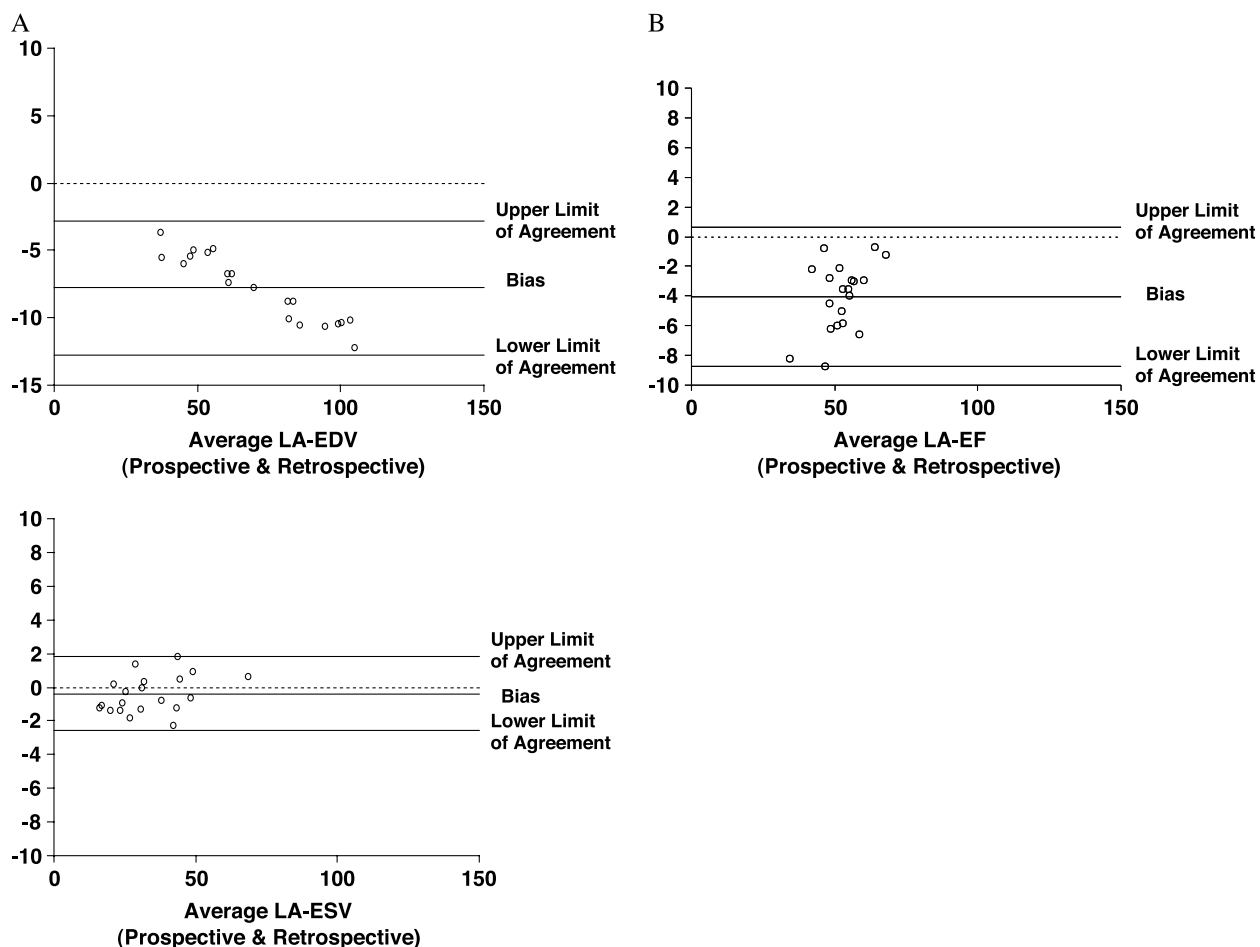


Figure 3. Band-Altman analysis of the differences between left and right ventricular volumes (A) and EF (B) acquired with prospective triggering and retrospective gating.

Table 2. Interobserver variability of the left (A) and right (B) ventricular volumes and EF measurements

	P-value	95% limits of agreement	
Table 2A			
Prospective triggering, mean difference			
EDV [mL]	-0.6 ± 3.6	0.52	-7.8, 6.6
ESV [mL]	-0.4 ± 2.0	0.45	-4.4, 3.6
SV [mL]	-0.13 ± 2.1	0.81	-4.3, 4.1
EF [%]	0.2 ± 1.1	0.48	-2.0, 2.4
Retrospective gating, mean difference			
EDV [mL]	0.6 ± 4.0	0.57	-7.4, 8.6
ESV [mL]	-0.67 ± 3.6	0.49	-7.9, 6.6
SV [mL]	1.2 ± 4.4	0.31	-7.7, 10.1
EF [%]	0.2 ± 2.5	0.76	-4.8, 5.2
Table 2B			
Prospective triggering, mean difference			
EDV [mL]	-0.67 ± 3.3	0.44	-7.2, 5.9
ESV [mL]	-0.67 ± 2.2	0.26	-5.0, 3.7
SV [mL]	-0.13 ± 1.7	0.76	-3.5, 3.2
EF [%]	0.4 ± 1.2	0.23	-2.1, 2.9
Retrospective gating, mean difference			
EDV [mL]	2.07 ± 4.1	0.07	-6.1, 10.2
ESV [mL]	1.0 ± 3.6	0.30	-6.2, 8.2
SV [mL]	1.07 ± 2.8	0.16	-4.5, 6.7
EF [%]	-0.4 ± 2.2	0.49	-4.8, 4.0

$p < 0.0001$; EDV right: 14.2 ± 3.9 mL, $p < 0.0001$; SV right: 14.7 ± 5.9 mL, $p < 0.0001$), Table 1. EF was significantly smaller with the prospectively triggered SSFP sequence for both right (mean difference: $3.6 \pm 3.3\%$, $p = 0.0008$) and left ventricle (mean difference: $2.3 \pm 3.3\%$, $p = 0.02$). Left and right ventricular ESV remained unchanged (mean difference: ESV left: 0.47 ± 3.5 mL, $p = 0.6179$; right ESV: 0.5 ± 3.7 mL, $p = 0.6083$). The Bland-Altman analysis of the differences between left and right ventricular volumes and EF acquired with prospective triggering and retrospective gating are displayed in Fig. 3.

The interobserver variability for left and right ventricular volumes and EF is displayed in Table 2.

4. Discussion

Cardiovascular magnetic resonance imaging (CMR) allows accurate and reproducible evaluation of left and right ventricular function and determination of left and right ventricular volumes and ejection fraction (7–12). Because of rapid technical advances in the field of CMR, image acquisition with faster gradient-echo sequences has become possible. The advantages are a shorter breath hold period and greater temporal and spatial resolution, which results in better blood-myocardium contrast, and greatly facilitates the identification of the ventricular endocardium and epicardium.

For volumetric assessment, the right and left ventricles are imaged in slices at fixed intervals from the base (atrioventricular ring) to the apex. The surface contours of the endocardium and epicardium are delineated (Fig. 1) and the ventricular volumes derived by summation with the assistance of computer software.

Using prospectively triggered image sequences, the acquisition window has to be set 10–20% below the average cycle length. Therefore, only 80–90% of the entire cardiac cycle is covered and is available for data analysis (Figs. 1 and 4). Due to the fact that no data is recorded for the remaining 10–20% of the cardiac cycle, the late diastole, EDV calculated from images acquired with a prospectively triggered gradient-echo sequence may be underestimated. This might result in significant differences in SV and EF.

We therefore addressed the question of whether the gating method significantly influences ventricular volume and EF measurements.

We found that EDV, SV, and EF differ significantly depending on the gating method used for image acquisition. The global EF is underestimated by the prospective triggering method. The values for ESV remained unchanged for both ventricles regardless of the gating method used for image acquisition. The difference of the results between the two gating methods is explained by the fact that the late diastole is not covered by prospective triggering, whereas the entire

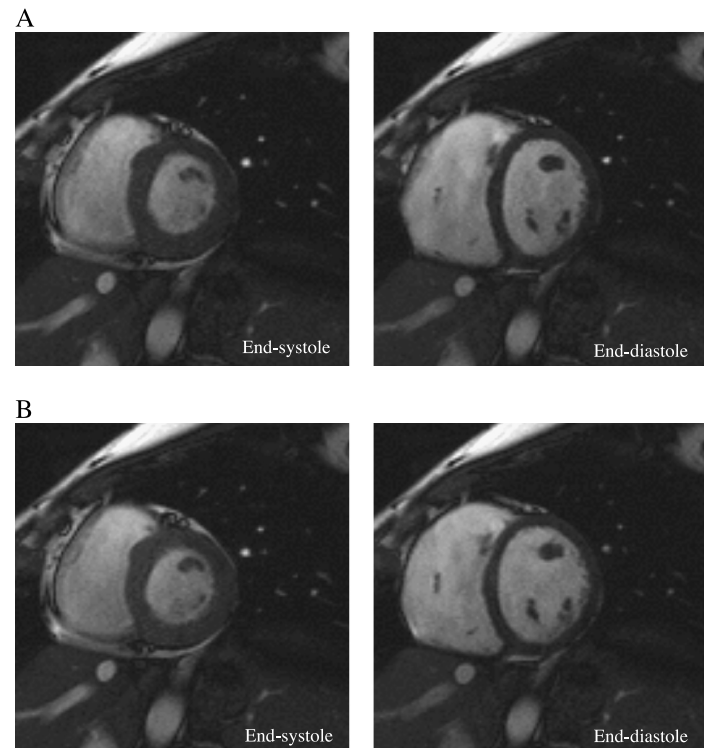


Figure 4. Mid-ventricular short-axis image acquired with a prospectively triggered SSFP sequence (A) and a retrospectively gated SSFP sequence (B). The left and right ventricles are larger in B (end-diastole).

cardiac cycle is covered by retrospective gating. Therefore, differences in EDV, but not in ESV are expected. However, the differences in left ventricular EF ($-2.3 \pm 3.3\%$, $p = 0.02$) are small and may not be of clinical relevance, although they were significant. The difference for the right ventricle is larger ($-3.6 \pm 3.3\%$, $p = 0.0008$). That might be explained in part by partial volume effects resulting from through-plane motion effects due to extensive longitudinal systolic contraction and diastolic relaxation of the non-elliptical shaped right ventricle.

Because of the over-sampling required for the retrospective gating method, the scan parameters were different between the two acquisitions. The spatial resolution was better in the prospectively triggered sequence than in the retrospectively gated sequence. The matrix size of the retrospectively gated sequence was reduced to avoid intolerable breath-hold durations. The scan parameters were optimized for the sequence and gating method to get the best image quality within a reasonable breath-hold time. However, the differences in the parameter setting could potentially have affected the results.

Retrospective gating is recommended for patients with irregular cardiac cycles, due to frequent premature beats and other kind of arrhythmias.

However, we did not attempt to study the difference in volumes and EF between these two gating techniques in patients with irregular heartbeats. We wanted to point out the difference in volumes and EF in subjects with normal sinus rhythm. In addition, the retrospectively gated SSFP sequence we used in our study was not very robust in patients with arrhythmias and the image quality was poor. This might be due to the fact that the sequence was not ECG triggered. First experiences with a recently developed retro-gated triggered SSFP sequence with arrhythmia rejection are very promising. Unfortunately, this sequence is currently only available for a few centers as a "work in progress package." Centers who have access to this improved sequence might be encouraged to address this issue.

MRI offers multiple different ways to change image and sequence settings. Differences in sequence as well as in parameter settings may result in different study results. As yet no standardized parameter setting for image acquisition and volume and EF assessment has been established. Therefore, imaging and sequence parameters need to be taken into account when using published data for reference values to distinguish between normal and abnormal. The gating method has a significant impact on volume and EF measurements. The global ventricular EF is underestimated by the prospectively triggered technique.

Acknowledgments

The authors thank Wolfgang Rehwald, Ph.D., for his helpful comments on the manuscript.

References

1. Salton CJ, Chuang ML, O'Donnell CJ, Kupka MJ, Larson MG, Kissinger KV, Edelman RR, Levy D, Manning WJ. Gender differences and normal left ventricular anatomy in an adult population free of hypertension. A cardiovascular magnetic resonance study of the Framingham heart study offspring cohort. *J Am Coll Cardiol* 2002; 39(6):1055–1056.
2. Alfakih K, Plein S, Thiele H, Jones T, Ridgway JP, Sivanathan MU. Normal human left and right ventricular dimensions for MRI as assessed by turbo gradient echo and steady-state free precession imaging sequences. *J Magn Reson Imaging* 2003; 17(3):323–329.
3. Lenz GW, Haacke EM, White RD. Retrospective cardiac gating: a review of technical aspects and future directions. *Magn Reson Imaging* 1989; 7(5):445–455.
4. Brown MA, Semelka RC. MR imaging abbreviations, definitions and descriptions: a review. *Radiology* 1999; 213:647–662.
5. Lorenz CH, Walker ES, Morgan VL, Klein SS, Graham TP Jr. Normal human right and left ventricular mass, systolic function, and gender differences by cine magnetic resonance imaging. *J Cardiovasc Magn Reson* 1999; 1(1):7–21.
6. Bland JM, Altman DG. Statistical methods for assessing agreement between two methods of clinical measurement. *Lancet* 1986; 1(8476):307–310.
7. Pattynama PM, Lamb HJ, Van der Velde EA, Van der Geest RJ, van der Wall EE, de Roos A. Reproducibility of magnetic resonance imaging-derived measurements of right ventricular volumes and myocardial mass. *Magn Reson Imaging* 1995; 13:53–63.
8. Sakuma H, Fujita N, Foo TK, Caputo GR, Nelson SJ, Hartiala J, Shimakawa A, Higgins CB. Evaluation of left ventricular volume and mass with breath-hold cine MR imaging. *Radiology* 1993; 188:371–376.
9. Dulce MC, Mostbeck GH, Friese KK, Caputo GR, Higgins CB. Quantification of the left ventricular volumes and function with cine MR imaging: comparison of geometric models with three-dimensional data. *Radiology* 1993; 188:37–371.
10. Sakuma H, Globits S, Bourne MW, Shimakawa A, Foo TK, Higgins CB. Improved reproducibility in measuring LV volumes and mass using multicoil breath-hold cine MR imaging. *J Magn Reson Imaging* 1996; 1:124–127.
11. Grothues F, Smith GC, Moon JC, Bellenger NG, Collins P, Klein HU, Pennell DJ. Comparison of interstudy reproducibility of cardiovascular magnetic resonance with two-dimensional echocardiography in normal subjects and in patients with heart failure or left ventricular hypertrophy. *Am J Cardiol* 2002; 90(1):29–34.
12. Grothues F, Moon JC, Bellenger NG, Smith GS, Klein HU, Pennell DJ. Interstudy reproducibility of right ventricular volumes, function, and mass with cardiovascular magnetic resonance. *Am Heart J* 2004; 147(2):218–223.

Copyright of Journal of Cardiovascular Magnetic Resonance is the property of Marcel Dekker Inc. and its content may not be copied or emailed to multiple sites or posted to a listserv without the copyright holder's express written permission. However, users may print, download, or email articles for individual use.